中國機械工程學刊第四十四卷第六期第 565~572 頁(民國一百一十二年)
Journal of the Chinese Society of Mechanical Engineers, Vol.44, No.6, pp565~572 (2023)

Study on The Journal Center Orbit of Micro-Polar Lubricated Offset-Halves Journal Bearings

Lili Wang*, Longchao Li**, Jingdong Duan** and Yunlong Bao**

Keywords: micropolar lubrication, offset-halves journal bearing, nonlinear journal center orbit, step and rectangular load.

ABSTRACT

During the actual operation, bearings are inevitably subjected to various loads, and the journal center orbit shows many lubrication patterns, the transient performance of the journal center orbit of micro-polar lubricated offset-halves journal bearings is studied. A nonlinear journal center orbit calculation model is established, the Eulerian method is applied to calculate the journal center orbit, and the journal center orbit and bearing lubrication performance under step load and rectangular load are studied. The results show that the action time of rectangular load is limited, and the journal center converges to the original equilibrium position after the load disappears, while the journal center converges to the new equilibrium position when the step load is applied. When the bearing is subjected to transient load, the oil film thickness and pressure will produce large change, and the oil film thickness and pressure will return to the previous state as the load disappears. The oil film pressure of the upper and lower bushes of the offset-halves journal bearing is equal in values and opposite in direction without load. The pressure of the lower bush increases and the pressure of the upper bush decreases while loading.

INTRODUCTION

With the rapid development of modern industry, rotating machinery shows the development trend of high speed, precision and heavy load. The bearings are subjected to various complex loads during operation, resulting in change in the operating condition of the bearings. In the spindle-rotor system, the journal center orbit of the spindle-rotor reflects the information of the working condition, internal lubrication condition and minimum oil film thickness of the bearing. Moreover, in machine tool machining, high precision machining of non-circular rotary surfaces can be achieved, by applying a control force to the journal bearing and make the bearing spindle move according to a predetermined trajectory. Therefore, the study of the journal center trajectory has the important theoretical significance and application value.

From the working principle, researchers have studied the axial trajectories of hydrostatic journal bearings, hydrodynamic journal bearings and hybrid journal bearings. Hu et al. (2018) calculated the journal center orbit of hydrostatic bearing according to the Eulerian method, and analyzed the effect of bearing width-to-diameter ratio and radius clearance on the journal center orbit. Guo et al. (2020) compared the dynamic contact force and journal center orbit in the start-up stage considering the thermal effect model with the isothermal model. Yang (2022) obtained the nonlinear oil-film forces by solving the Reynolds equation with bearing waviness based on the finite difference method. Hou et al. (2021) conducted an experimental study on the journal center orbit of a twin-screw refrigeration compressor rotor. He (2013) studied the hydrostatic bearing with four oil recesses with oil return grooves, and found that the equilibrium position of the capillary throttled hydrostatic bearing journal center trajectory gradually approached the center of origin with the increase of speed. Ma (2022) studied the journal center orbit of a stress-coupled fluid-lubricated bearing, and compared the axis center orbit of stress-coupled fluid lubrication with that of Newtonian fluid lubrication. Cui et al. (2018, 2018) studied the effect of surface roughness and radius clearance on the transient characteristics of axis center orbit under mixed lubrication condition during bearing start-up.

Paper Received March, 2023. Revised May, 2023. Accepted July, 2023. Author for Correspondence: Lili Wang.

* *Associate Professor, College of Mechanical and Electronic Engineering, Shandong University of Science and Technology, Qingdao, China 266590.*

** *Graduate Student, College of Mechanical and Electronic Engineering, Shandong University of Science and Technology, Qingdao, China 266590.*

In order to improve the bearing performance, researchers have investigated the journal center orbit under different bearing lubricants. Cao et al. (2022) studied the journal center orbit and lubrication performance of water-lubricated bearings in the starting process under various roughness. Shi (2021) studied the journal center orbit of a hemispherical spiral groove gas bearing under horizontal starting condition, and found that the sphericity error had little effect on the bearing starting process. In order to meet the development of modern industry and improve the stability of the bearing, lubricants are added with some additives, which can be considered as the suspended tiny particles, is called the micropolar fluid. Manser et al. (2020) used a micropolar fluid model to calculate the static performance of a finite-width journal bearing, micropolar fluids significantly improved the load capacity and friction force at high eccentricity, high coupling number, and low characteristic length. Wang et al. (2020) analyzed the hydrodynamic behavior of slider bearings, as the micro-rotational and angular viscosities decrease, the hydrodynamic behavior of micropolar fluids will gradually approach the classical Newtonian fluid. Liang et al. (2022) studied the journal center orbit during the start-up of water-lubricated bearings in ship propulsion systems, and analyzed the effect of the magnitude, direction and entry time of wave on the starting performance of the bearings. Kumar et al. (2020) found that the static and dynamic performance of the bearings was greatly improved when non-Newtonian lubricants were used. Zhang et al. (2012) approached the rotor system, bearing housings and nonlinear fluid films using the finite element method. Sharma et al. (2022) showed that the micro-polar lubricated offset bearing had higher stability, smaller characteristic length and higher dam width performance than conventional bearings. Airton et al. (2021) established the finite element model of the nonlinear formulation of a magnetorheological fluid journal bearing. Bhattacharjee (2022) investigated and compared the steady-state performance of micropolar fluid lubricated single-layered and double-layered porous journal bearings. Considered rough surface and squeezing action, Naduvinamani (2022) investigated the dynamic characteristics of porous inclined slider bearing with micropolar fluid lubricant.

It is found that the offset bearings are simple in structure and show greater advantages in stability than conventional bearings. Chourasia (2022) carried out the static analysis and modal analysis of bearings made of structural steel, gray cast iron, aluminum alloy. The lubrication performance of journal center orbit or micro-polar lubricated hydrodynamic offset bearing has been studied, the journal center orbit of micro-polar lubricated hydrodynamic offset bearing is studied in the paper, the journal center orbit contains a lot of information of the bearing, it is of important significance to the control of the journal center orbit, and high precision machining of non-circular rotary surfaces.

CALCULATION MODELING OF NONLINEAR JOURNAL CENTER ORBIT

Oil film thickness

Figure 1 shows the sketch of oil film thickness calculation, the starting angle φ starts from the negative half-axis of x-axis, O_j is the journal center, O is the bearing center, O_1 is the center of lower bush, and O_2 is the center of upper bush. h of the bearing can be expressed as

$$h = c + e\sin(\varphi - \theta) \pm (c - c_m)\cos\varphi \tag{1}$$

where c_m is the minimum radial clearance, c is the radial clearance, e is the eccentricity, φ is the calculated starting angle, θ is the attitude angle.

Introducing dimensionless variables $\overline{h} = \frac{h}{c_m}$, $\frac{1}{\delta} = \frac{c}{c_m}$, $\varepsilon = \frac{e}{c_m}$ the dimensionless equation of the oil film thickness can be obtained as

$$\overline{h} = \frac{1}{\delta} + \varepsilon\sin\theta\cos\varphi + \varepsilon\cos\theta\sin\varphi \pm \frac{1-\delta}{\delta}\cos\varphi \tag{2}$$

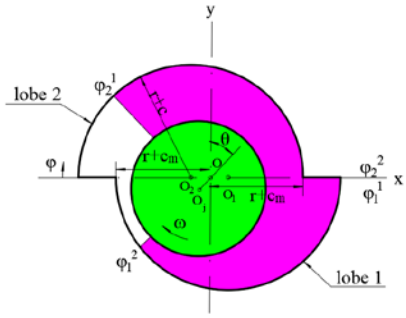

Figure. 1 Sketch of oil film thickness calculation

If the axial coordinates are denoted by (x_j, y_j), $e = \sqrt{x_j^{\,2} + y_j^{\,2}}, x_j = e\sin\theta, y_j = -e\cos\theta,$ $(X_j, Y_j) = \frac{(x_j, y_j)}{c_m} = (\varepsilon\sin\theta, -\varepsilon\cos\theta)$, the dimensionless oil film thickness can be expressed as (Sharma, 2022)

$$\overline{h} = \frac{1}{\delta} + X_j\cos\varphi - Y_j\sin\varphi \pm \frac{1-\delta}{\delta}\cos\varphi \tag{3}$$

Reynolds equation of micropolar fluids

The modified Reynolds equation of the micropolar fluid lubricated, incompressible, laminar flow state is as following (Das, 2004)

$$\frac{\partial}{\partial x}\left(\frac{\psi(N,\Lambda,h)}{u}\frac{\partial p}{\partial x}\right)+\frac{\partial}{\partial y}\left(\frac{\psi(N,\Lambda,h)}{u}\frac{\partial p}{\partial y}\right)=6U\frac{\partial h}{\partial x}+12\frac{\partial h}{\partial t} \quad (4)$$

where $\psi(N,\Lambda,h)=h^3+12\Lambda^2 h-6N\Lambda h^2\coth\left(\frac{Nh}{2\Lambda}\right)$, $\Lambda=\left(\frac{C_a+C_d}{4u}\right)^{\frac{1}{2}}$, $N=\left(\frac{u_r}{u+u_r}\right)^{\frac{1}{2}}$, C_a and C_d are the angular velocity coefficient, u is the Newtonian hydrodynamic viscosity, u_r is the dynamic micro-rotational viscosity, h is the fluid film thickness, U is the axial linear velocity, t is the time. Introducing dimensionless variables

$\varphi=\frac{x}{r},\lambda=\frac{y}{L},\bar{p}=\frac{p}{Uur}$,

$(\dot{X}_j,\dot{Y}_j)=\frac{(\dot{x}_j,\dot{y}_j)}{c_m\omega},\tau=\omega t, lm=\frac{c_m}{\Lambda}$, the dimensionless form of equation (4) is as following

$$\frac{\partial}{\partial x}\left(\frac{\psi(N,lm,\bar{h})}{u}\frac{\partial\bar{p}}{\partial\varphi}\right)+\left(\frac{r}{l}\right)^2\frac{\partial}{\partial\lambda}\left(\frac{\psi(N,lm,\bar{h})}{u}\frac{\partial\bar{p}}{\partial\lambda}\right)= 6\frac{\partial\bar{h}}{\partial\varphi}+12\frac{\partial\bar{h}}{\partial\tau} \quad (5)$$

where r is the journal radius.

The variation of oil film thickness with τ is as following

$$\frac{\partial\bar{h}}{\partial\tau}=\dot{X}_j\cos\varphi-\dot{Y}_j\sin\varphi \quad (6)$$

The equations for the bearing capacity in horizontal and vertical directions (Rahmatabadi, 2010) are as following

$$\begin{Bmatrix}\overline{W_x}\\ \overline{W_y}\end{Bmatrix}=\sum_{i=1}^{2}\begin{Bmatrix}\overline{W_x}^i\\ \overline{W_y}^i\end{Bmatrix}= -\sum_{i=1}^{2}\int_{-1}^{1}\int_{\varphi_1^i}^{\varphi_2^i}\bar{P}_i d\lambda\begin{Bmatrix}\cos\varphi\\ \sin\varphi\end{Bmatrix}d\varphi \quad (7)$$

where i =1 represents the lower bush, i=2 represents the upper bush.

Motion equations of the nonlinear journal center orbit

The offset-halves journal bearing calculation model is shown in Figure 2. W_{x2} and W_{x1} are oil film force of the upper and lower bush in the x direction, respectively, W_{y2} and W_{y1} are oil film force of the upper and lower bush in the y direction, respectively, Q_x and Q_y are the load components acting on the axis in the x and y directions, Mg is the weight of the axis, the equation of motion of the axis can be obtained according to Newton's second law of motion.

$$\begin{cases}M\ddot{x}_j=W_{x1}+W_{x2}+Q_x\\ M\ddot{y}_j=W_{y1}+W_{y2}-Q_y-Mg\end{cases} \quad (8)$$

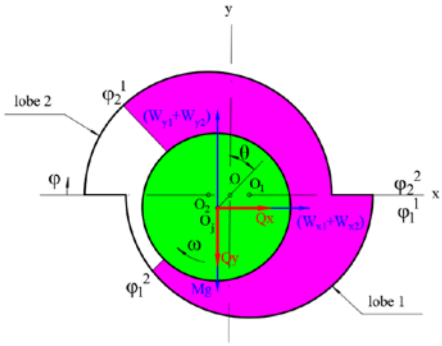

Figure. 2 Bearing calculation model

The dimensionless form is obtained by dividing both sides of the equation (7) simultaneously by $Mc_m\omega^2$.

$$\begin{Bmatrix}\ddot{X}_j=\alpha(W_{x1}+W_{x2})+Q_x\\ \ddot{Y}_j=\alpha(W_{y1}+W_{y2})-Q_y-\beta\end{Bmatrix} \quad (9)$$

where $\ddot{X}_j=\frac{\ddot{x}_j}{c_m\omega^2},\ddot{Y}_j=\frac{\ddot{y}_j}{c_m\omega^2},\alpha=\frac{uLr^3}{Mc_m^3\omega}$,

$\overline{W_{x1}}=\frac{W_{x1}c_m^2}{uL\omega r^3},\overline{W_{x2}}=\frac{W_{x2}c_m^2}{uL\omega r^3},\overline{W_{y1}}=\frac{W_{y1}c_m^2}{uL\omega r^3},\overline{W_{y2}}=\frac{W_{y2}c_m^2}{uL\omega r^3}$,

$\overline{Q_x}=\frac{Q_x}{Mc_m\omega^2},\overline{Q_y}=\frac{Q_y}{Mc_m\omega^2},\beta=\frac{g}{c_m\omega^2}$.

Calculation of nonlinear journal center movement orbit

Calculation modeling of nonlinear journal center orbit includes the oil film thickness Equation (3), the modified Reynolds Equation (5), the equations for the bearing capacity (7), the motion equation of the axis (8). The specific calculation process is as follows:

Calculating the journal center orbit of the journal bearing, it is necessary to first calculate the oil film thickness Eq. (3) for the initial position to get the oil film thickness distribution of the bearing, the initial journal position and velocity are generally set to 0 (the change in initial value does not affect the convergence result as shown in the reference (Ma, 2010), the modified Reynolds Eq. (5) under micro-polar fluid lubrication is solved to get the pressure distribution of bearing, the oil film component force is gained by the integral of Eq. (7), the axial acceleration is solved by the equation of motion (8), the axial position and velocity of the next moment are calculated by the Equation (10) according to Euler's method, and then the oil film thickness equation of the moment is recalculated, this is repeated until the journal center orbit in a given time is calculated.

$$\left\{\begin{array}{l} \dot{X}_j(\tau+\Delta\tau)=\dot{X}_j(\tau)+\ddot{X}(\tau)\Delta\tau \\ X_j(\tau+\Delta\tau)=X_j(\tau)+\dot{X}(\tau+\Delta\tau)\Delta\tau \\ \dot{Y}_j(\tau+\Delta\tau)=\dot{Y}_j(\tau)+\ddot{Y}(\tau)\Delta\tau \\ Y_j(\tau+\Delta\tau)=Y_j(\tau)+\dot{Y}(\tau+\Delta\tau)\Delta\tau \end{array}\right\} \tag{10}$$

RESULTS AND ANALYSIS

Calculated parameters

The bearing parameters are shown in Table 1, which are used to calculate the nonlinear journal center orbit with a misalignment factor δ of 0.5 and a calculation time t of 0.25s. The dimensionless time $\tau=\omega t=100\pi\times 0.25=78.5398$, α and β in Equation (9) are calculated as 53.0581 and 1.9095.

Table 1 Bearing parameters

Name	Symbol	Value	Unit
Bearing length	L	0.025	m
Bearing radius	r	0.05	m
Minimum radius clearance	c_m	0.00025	m
Rotor mass	M	20	kg
Lubricant viscosity	u	0.015	Pa·s
Rotational Speed	n	3000	r/min
Calculation time	t	0.25	s
Radial clearance	c	0.0005	m

Journal center orbit under step load

Under actual working conditions, bearings are affected by transient loads, such as step load and rectangular load, etc. The paper focuses on the effect of step load and rectangular load on bearing lubrication performance. The step load is acted on the journal, the expression is as following:

$$\overline{Q_x}(\tau)=0$$

$$\overline{Q_y}(\tau)=\begin{cases}0, 0\le\tau\le 16\pi \\ 1, \tau\ge 16\pi\end{cases} \tag{11}$$

Figure 3 shows the change of the journal trajectory and bearing parameters of the offset-halves journal bearing under micro-polar lubrication, when the bearing is subjected to the step load. Fig. 3(a) shows the change of the journal center orbit and the pressure distribution in the initial position, the first equilibrium position and the second equilibrium position. At $\tau\le 16\pi$, the step load is zero, the resultant force of the oil film force, the journal gravity and the inertia force on the bearing is zero, the axial position is adjusted automatically from the initial position, and then converges to the first equilibrium position $X_j=-0.05998, Y_j=-0.29674$, which is the equilibrium position when the bearing only bears the weight of the journal, the inertia force on the bearing is zero, the bearing load of the upper and lower bushes is balanced with the journal gravity, and the bearing reaches the static equilibrium state. At $16\pi\le\tau<25\pi$, the bearing is subjected to the load $\overline{Q_y}=1$, the equilibrium state of the bearing is broken, the axis begins to automatically adjust, and convergences to the second equilibrium position $X_j=-0.0742, Y_j=-0.43648$,from the first equilibrium position; then the bearing inertia force again becomes zero, the resultant force of the bearing upper and lower bush is balanced with the resultant force of journal gravity and step load, the bearing reaches a new equilibrium state. When the journal center is in the initial position, the journal center coincides with the bearing center, the bearing upper and lower bushes form two oil wedges with equal pressure in opposite directions.

Fig. 3(b) shows the variation of dimensionless minimum oil film thickness with dimensionless time τ. When there is no load (τ=0), the journal diameter is located in the geometric center of the bearing, and the minimum oil film thickness of the upper and lower bushes of the bearing is equal; after being loaded by the journal weight itself, the journal center moves downward, the minimum oil film thickness of the upper bush increases, and the minimum oil film thickness of the lower bush decreases; after being subjected to the step load, the journal center will continue to move downward, minimum oil film thickness and maximum oil film pressure have significant changes and exhibit a certain oscillation process, which also reflects the automatic centering mechanism of the bearing. The minimum oil film thickness of the upper bush increases from 1.0599 to 1.0742, the minimum oil film thickness of the lower bush decreases from 0.8996 to 0.8405. The change of oil film thickness will cause the change of bearing pressure, as shown in Fig. 3(c), the dimensionless maximum oil film pressure of upper bush increases from 0.0726 to 0.07425, and the dimensionless maximum oil film pressure of lower bush increases from 0.11167 to 0.13708. Fig. 3(d) shows the change of axial displacement X_j, Y_j with dimensionless time τ, the displacement in Y direction after adding the step load has a larger change, which is because the load becomes larger, the bearing will increase the eccentricity to balance the external load, the change of eccentricity causes the change of circumferential pressure, the attitude angle will also change in order to meet the requirement of external load, so the axial

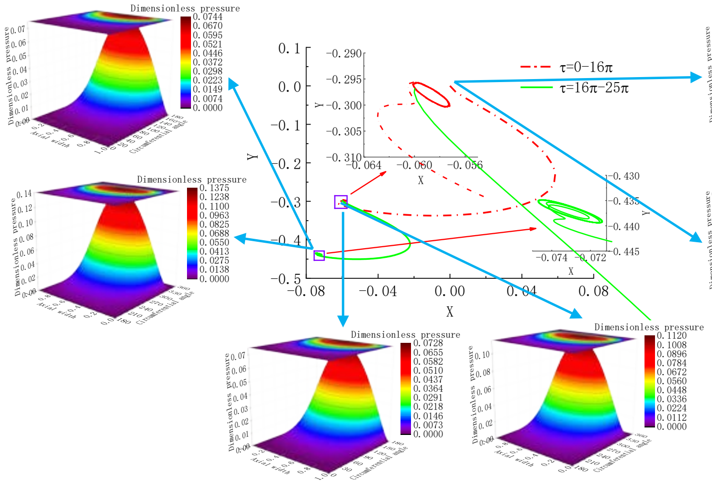

(a) Journal center orbit

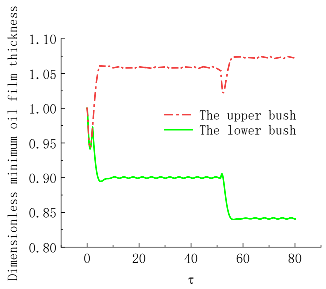

(b) Minimum oil film thickness with time τ

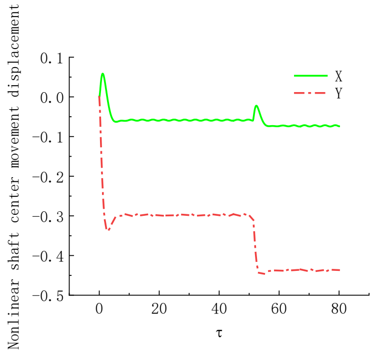

(d) Axial nonlinear displacement with time τ

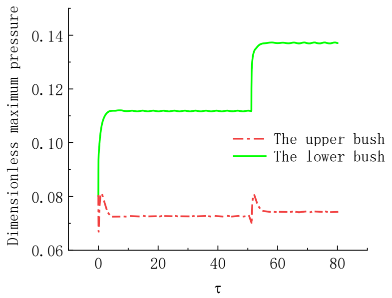

(c) Maximum oil film pressure with time τ

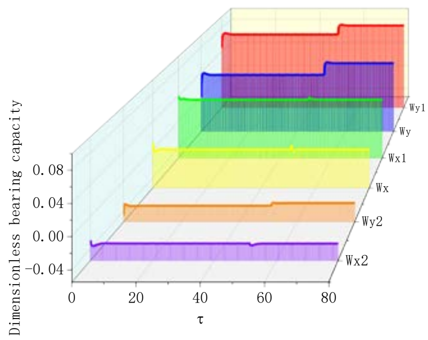

(e) Dimensionless load carrying capacity with time τ

Figure. 3 Variation of bearing parameters under step load displacement in the X direction will also change, which is consistent with the trend of the journal center movement orbit in the reference (Ma, 2010). Fig. 3(e) is the variation of the dimensionless oil film force with the dimensionless time τ. It can be found that after the step load is loaded on the Y direction, in order to resist the external load, the oil film force of the upper bush, the oil film partition force of the lower bush and the oil film consultant force in the Y direction produce a large change; and because there is no load in the X direction, the oil film force of the upper bush, the oil film force of the lower bush and the oil film consultant force in X-direction remain basically unchanged.

Journal center orbit under rectangular load

The rectangular load is acted on the bearing, the expression is as following:

$$\overline{Q}_x(\tau) = 0$$

$$\overline{Q}_y(\tau) = \begin{cases} 0, 0 \le \tau < 16\pi \\ 1, 16\pi \le \tau < 18\pi \\ 0, \tau \ge 18\pi \end{cases} \tag{12}$$

The effect of unidirectional rectangular pulse load on the journal center orbit and lubrication performance of the micropolar lubricated offset-halves journal bearing is shown in Figure 4. Fig. 4(a) shows the oil film pressure of the journal center orbit and stable position within the dimensionless time $\tau = 25\pi$. At $0 < \tau < 16\pi$, the bearing only bears the load of the journal weight and the axial center converges at $X_j = -0.05998$, $Y_j = -0.29674$. At $16\pi < \tau < 18\pi$, the bearing is subjected to the load $Q_y(\tau) = 1$ and the axial center convergences at $X_j = -0.0742, Y_j = -0.43648$, at this time, the rectangular load on the bearing is consistent with the step load, the convergence position of the axis is consistent with the step load ($\tau < 18\pi$). At $18\pi < \tau < 25\pi$, $Q_y(\tau) = 0$, the rectangular load disappears and the bearing starts to oscillate, and the bearing finally returns to the first equilibrium position again, but the journal center converges to the second equilibrium position when the step load is applied.

Fig. 4(b) is the variation of the dimensionless minimum oil film thickness with the dimensionless time, at the loading time ($16\pi < \tau < 18\pi$), the minimum oil film thickness of the bearing upper bush increases from 1.05998 to 1.07334, and the minimum oil film thickness of the lower bush decreases from 0.89927 to 0.8405. After the rectangular load disappears, the bearing returns to the first equilibrium position. The maximum oil film pressure also changes, as shown in Fig. 4(c), as the rectangular load is applied, the oil film pressure increases in order to resist the rectangular load, the dimensionless maximum oil film pressure of upper bush increases from 0.07262 to 0.07431, and the dimensionless maximum oil film pressure of lower bush increases from 0.11174 to 0.13727, the maximum oil film pressure is consistent with the first equilibrium position after the rectangular load disappears. Fig. 4(d) is the change of axial displacement X_j, Y_j with dimensionless time τ, the rectangular load acts in Y direction, the displacement in Y direction changes more, which is the same as the step load, the attitude angle changes, the displacement in X direction also changes, but compared with the displacement in Y direction does not change much, the displacement in X and Y direction is again consistent with the first equilibrium position after the load disappears. Fig. 4(e) shows the variation of dimensionless carrying capacity with dimensionless time under rectangular load, which is similar to the step load, in order to resist the external load, the oil film force of the upper bush, the oil film force of the lower bush, the oil film resultant force in the Y direction all produce the larger change; there is no load in the X direction, the oil film force of the upper bush, the oil film force of the lower bush, and the oil film resultant force in the X direction are basically unchanged. After the rectangular load disappears, the bearing capacity returns to the carrying capacity of the first equilibrium position.

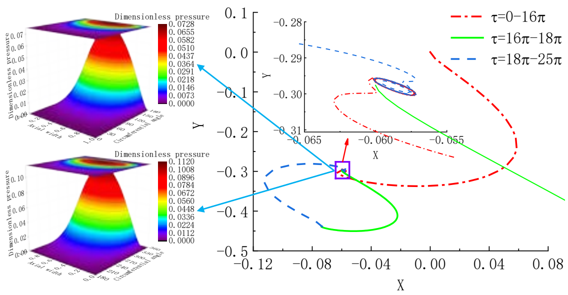

(a) Journal center orbit

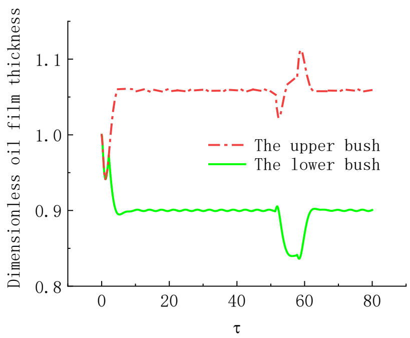

(b) Minimum oil film thickness with time τ

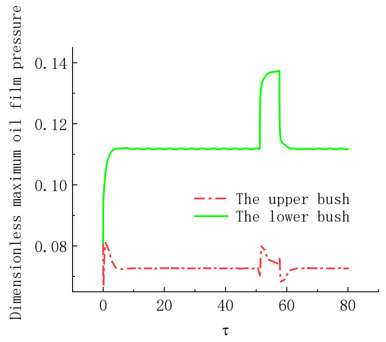

(c) Maximum oil film pressure with time τ

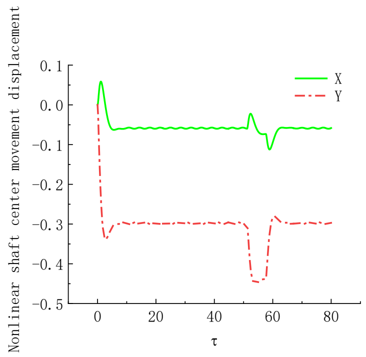

(d) Axial nonlinear displacement with time τ

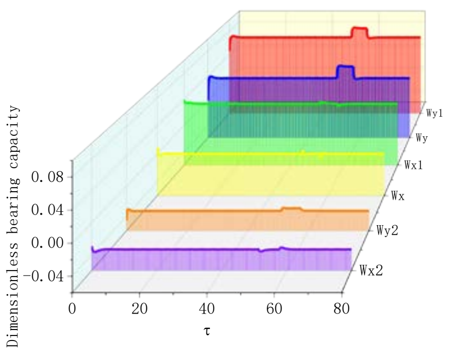

(e) Dimensionless load carrying capacity with time τ

Figure 4 Variation of bearing parameters under rectangular load

CONCLUSIONS

Using the equilibrium between oil film force, inertia force and external load, a nonlinear journal center orbit calculation model is established, and the change of journal center orbit, minimum oil film thickness, maximum oil film pressure, axial displacement and oil film force under step load and rectangular load are calculated, and the main conclusions are as follows:

The action time of rectangular load is limited, and the journal center still converges to the original equilibrium position after the load disappears, and the journal center converges to the new equilibrium position when the step load is applied.

When the bearing is subjected to load, the journal center moves downward, the minimum oil film thickness of upper bush increases and the maximum oil film pressure decreases, the minimum oil film thickness of lower bush decreases and the maximum oil film pressure increases. After reaching the new equilibrium position, the oil film thickness and oil film pressure under step load cannot change; but the oil film thickness and oil film pressure will return to the first equilibrium position state under rectangular load after stabilizing for a period of time.

When there is no load, the oil film pressure of the upper and lower bushes of the offset-halves journal bearing is equal and opposite in direction, the upper bush pressure is not conducive to bearing load. When load is applied to the bearing, the lower bush pressure increases and the upper bush pressure decreases.

ACKNOWLEDGMENT

This work was supported by Shandong Province Key Laboratory of Mine Mechanical Engineering, Shandong University of Science and Technology (2022KLMM304), Qingdao Postdoctoral Research funded project.

REFERENCES

Airton, N. and Gustavo, F.F., “Nonlinear modeling and analysis of rotors supported by magnetorheological squeeze film journal bearings,” *Meccanica*, Vol.56, pp.873-886(2021).

Bhattacharjee, B., Biswas, N. and et al, “A comparative analysis of the performance of micropolar fluid lubricated single-layered and double-layered porous journal bearing,” *Journal of Porous Media*, Vol.25, No.9, pp. 35-45(2022).

Cao, Y. Z., Liang, P. and et al, “Effects of Surface Roughness on Transient Performance of Water Lubricated Bearings During Start-Up under Different Working Conditions,” *Journal of Propulsion Technology*, Vol.43, No.7, pp. 457-469(2022).

Chourasia, K. and Joladarashi, S., “Modelling, static and dynamic analysis of offset bearing using ANSYS,” *Materials Today: Proceedings*, Vol. 66, No.4, pp. 2124-2132(2022).

Cui, S., Gu, L. and et al, “The effects of surface roughness on the transient characteristics of hydrodynamic cylindrical bearings during startup," *Tribology International*, Vol.128, pp. 421-428(2018).

Cui, S., Gu, L. and et al, "Numerical analysis on the dynamic contact behavior of hydrodynamic journal bearings during start-up," *Tribology International*, Vol.121, pp. 260-268 (2018).

Das, S., Guha, S.K. and Chattopadhyay, A.K., "Theoretical analysis of stability characteristics of hydrodynamic journal bearings lubricated with micropolar fluids," *Journal of Engineering Tribology*, Vol.218, No.1, pp. 45-56(2004).

He, Y.L., "Calculation and Simulation of the Hybrid Bearings Nonlinear Centre Trajectory," *Shandong University* (2013).

Hou, F., Yang, C. and et al, "Experimental study of the fluctuation characteristics of axis orbit of rotors in twin-screw refrigeration compressor," *Fluid Machinery*, Vol.49, No.1, pp.16-21+28(2021).

Hu, B. L., Xiong, Y.P. and et al, "Study on the factors influencing the axis trajectory of liquid hydrostatic electric spindle," *Mechanical Engineering and Technology*, Vol.7, pp. 487(2018).

Kumar, S., Kumar, V. and Singh, A. K., "Influence of lubricants on the performance of journal bearings–a review," *Tribology-Materials, Surfaces & Interfaces*, Vol.14, No.2, pp. 67-78(2020).

Liang, P., Li, X. and et al, "Influence of sea wave shock on transient start-up performance of water-lubricated bearing," *Tribology International*, Vol.167, pp. 107332(2022).

Ma, J.K, "Study on transient and periodic characteristics of nonlinear journal center motion trajectories of journal bearing," *Shandong University* (2010).

Ma, Y.Y., "Calculation of Oil Film Pressure and Axis Orbit for Journal Bearings Lubricated with Couple Stress Fluids," *Lubrication Engineering*No.13, pp.1-6(2022).

Manser, B., Belaidi, I. and et al, "Computational investigation on the performance of hydrodynamic micro-textured journal bearing lubricated with micropolar fluid using mass-conserving numerical approach," *Journal of Engineering Tribology*, Vol.234, No.8, pp.1310-1331(2020).

NB, N. and Angadi, A., "On the Dynamic Characteristics of Rough Porous Inclined Slider Bearing Lubricated with Micropolar Fluid," *Tribology Online*, Vol.17, No.1, pp.59-70(2022).

Rahmatabadi, A.D., Nekoeimehr, M. and Rashidi, R., "Micropolar lubricant effects on the performance of noncircular lobed bearings," *Tribology International*, Vol.43, No.1-2, pp. 404-413(2010).

Sharma, S. and Krishna, C.M., "Static and dynamic performances of an offset bearing under a micropolar lubricant," *Journal of Engineering Tribology*, Vol.236, No.1, pp. 59-69(2022).

Sharma, S., Krishna, C.M. and Singh, R., "Analysis of elliptical dam bearing lubricated with micropolar fluid," *Industrial Lubrication and Tribology*, Vol.74, No.2, pp. 243-250(2022).

Shi, Y., "Study on start-up behavior of hemispherical spiral-grooved gas bearings," *Harbin Institute of Technology* (2021).

Wang, L., Chu, X. and et al, "Implementation of micropolar fluids model and hydrodynamic behavior analysis using user-defined function in FLUENT," *Advances in Mechanical Engineering*, Vol.12, No.7, pp.1-12(2020).

Xiang, G., Han, Y. and et al, "Transient tribo-dynamic model for journal bearings during start-up considering 3D thermal characteristic," *Tribology International*, Vol.144, pp.106123(2020).

Yang, J., Zhu, R.P. and et al, "Nonlinear analysis of herringbone gear rotor system based on the surface waviness excitation of journal bearing," *Journal of the Brazilian Society of Mechanical Sciences and Engineering*. Vol.44, No.2, pp.54(2022).

Zhang, H.F., Wu, J.H. and et al, "Transient Analysis of a Rotor-Journal Bearing System under Large and Dynamic Loads," *Journal of The Chinese of Mechanical Engineers*, Vol.33, No.4, pp.271-279(2012).